

Radiation measurements by a cryogenic *pn* junction InSb detector with operating temperatures up to 115 K

Ikuo Kanno,^{a)} Fumiki Yoshihara, and Ryo Nouchi
Graduate School of Engineering, Kyoto University, Sakyo, Kyoto 606-8501, Japan

Osamu Sugiura and Yasuhiro Murase
*Graduate School of Science and Engineering, Tokyo Institute of Technology, Meguro,
Tokyo 152-8552, Japan*

Tatsuya Nakamura and Masaki Katagiri
Japan Atomic Energy Research Institute, Tokai, Ibaraki 319-1195, Japan

(Received 2 December 2002; accepted 9 June 2003)

Pn junction-type radiation detectors were fabricated with an InSb substrate. The detectors had 1000 times higher resistances than those of previously reported Schottky-type detectors. The output pulses of the preamplifier were analyzed from the point of view of the contribution of electrons and holes. The energy spectra of ²⁴¹Am alpha particles were measured at operating temperatures of up to 115 K. The inherent voltage of the detector was estimated. © 2003 American Institute of Physics. [DOI: 10.1063/1.1599067]

I. INTRODUCTION

As x-ray detectors with high-energy resolution, superconducting detectors have been studied intensively. The superconducting radiation detectors are good at measuring x rays with energy of 6 keV, however, they have less efficiency for x rays with higher energies. For industrial applications and for materials science, the detection of x rays with energies higher than 6 keV is the main concern.

For the detection of high-energy photons, materials with a high atomic number, high density, and large active volume are necessary in order for their measurement to be made with high efficiency. Many kinds of compound semiconductors with the features described above, such as CdTe, have been developed. However, their band-gap energies are greater than the ones of conventional semiconductors, such as Si and Ge, with which detectors have been developed and widely employed, but are claimed to be short in energy resolution.

Among the compound semiconductor materials, InSb is the exception from the point of view of band-gap energy, as it has a smaller band-gap energy of 0.165 eV. This is $\frac{1}{6}$ of that of Si. This band-gap energy predicts that the energy resolution of a InSb detector is less than 60 eV for 6 keV x rays. In addition, the mobilities of electrons and holes of InSb are 78 000 and 750 cm² V⁻¹ s⁻¹, which are 40 and 1.5 times greater than the ones of Si, respectively. The high atomic number of In (49) and Sb (51), and its high density (5.78 g cm⁻³) make InSb a more attractive material for radiation detectors, especially for the measurements of high-energy photons. In this case we assume the figure of merit of photon absorption efficiency to be $Z^4\rho$, where Z and ρ are the atomic number and the density of detector material, respec-

tively, and InSb has 6.5 times greater absorption efficiency than Ge. This indicates that the InSb detector with a volume of 15 cc is equivalent to a Ge detector with a 100 cc volume, and has more than two times the energy resolution of the Ge detector.

McHarris has suggested the advantage of InSb as a substrate of photon detectors.¹ No work, however, has reported on InSb radiation detectors prior to the publication of our work.² In a previous article, we reported on the measurements of ²⁴¹Am alpha particles using a Schottky-type InSb detector. The current-voltage (I - V) curves, output pulses of the preamplifier, and the energy spectra of alpha particles were shown as a function of temperature. Although the detector was not at a stage where we were able to discuss its energy resolution, the InSb device worked as a radiation detector with changing responses according to the applied bias voltage and operating temperature.

In this article, we report on our second attempt to measure radiation by an InSb detector. Apart from the previous Schottky-type InSb detector, we fabricated *pn* junction-type InSb detectors. The fabrication method and electrical properties of this detector are shown. Based on the confirmation of the performance of the InSb detector at temperatures of 0.5 and 4.2 K, we concentrated on the measurement of alpha particles by the *pn* junction-type InSb detectors at higher operating temperatures of up to 115 K. The InSb detector showed a wide temperature operating range.

II. EXPERIMENT

A. Device fabrication

We fabricated the *pn* junction-type detectors on a *p*-type InSb substrate. The InSb wafer (Wafer Technology, Ltd., U.K.) had a diameter of 2 in., a thickness of 500 μ m, and a

^{a)}Electronic mail: kanno@qsec.kyoto-u.ac.jp

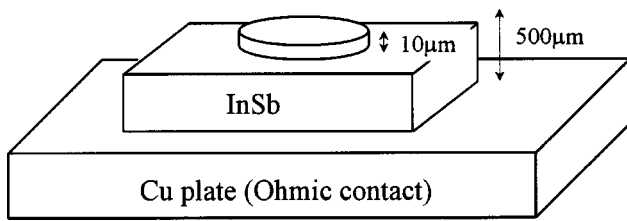


FIG. 1. Schematic drawing of the InSb detector.

Ge dopant concentration of $3.5 \times 10^{15} \text{ cm}^{-3}$. The resistivity of the InSb substrate at 77 K was $0.29 \text{ } \Omega \text{ cm}$.

Both sides of the InSb substrate (nearly $7 \text{ mm} \times 10 \text{ mm}$) were etched using a mixture of nitric and lactic acids (1:10) for 5 min. On the top side surface, Sn and Al were deposited by heat evaporation with thicknesses of nearly 5 nm and $0.1 \text{ } \mu\text{m}$, respectively. After evaporation, the Sn was diffused into the *p*-type InSb by lamp annealing and resulted in the *n*-type layer. After the definition of an electrode with a diameter of 3 mm by a photoresist mask, a mesa electrode was fabricated by etching. The height of the mesa was nearly $10 \text{ } \mu\text{m}$. Finally, the processed wafer was mounted on a Cu plate by silver paste having an Ohmic contact on the back surface. A schematic drawing of the detector is shown in Fig. 1.

B. Electric properties

Current–voltage curves measured by the same method as in the previous article are shown in Fig. 2. In this *pn* junction-type InSb detector, a nonlinearity is observed, even at an operating temperature of 77 K. A summary of the results of the resistances at voltages around 0 V and the voltage range for which the same resistance holds are shown in Fig. 3.

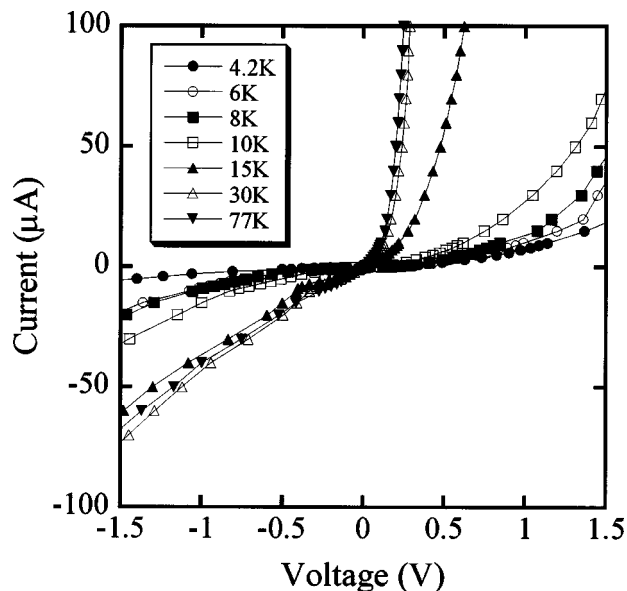


FIG. 2. Current–voltage curves of the InSb detector. The operating temperatures are shown in the figure.

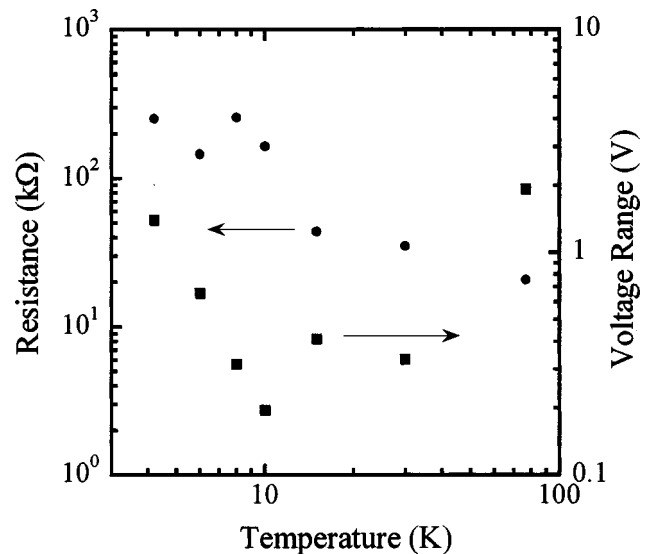


FIG. 3. Resistance (solid circles) and voltage range (solid squares) of the center regions of the *I*–*V* curves of Fig. 2.

C. Alpha particle measurement

Alpha particle measurements were carried out by the same method as described in Ref. 2. The InSb detector was mounted on the 0.3 K stage of a refrigerator (Infrared Co.) and an electro-deposited ^{241}Am alpha particle source ($25 \text{ } \mu\text{Ci}$) was placed some millimeters from the surface of the detector. The alpha particles (mainly 5.5 MeV in energy) were collimated at nearly 4 mm in diameter. The electronic circuit employed is also shown in Ref. 2. However, we would like to describe, again, that the voltage applied to the detector, V_d , was calculated using

$$V_d = V_i + \frac{R\Omega}{12\text{M}\Omega + R\Omega} V_b. \quad (1)$$

Here, V_i is the inherent voltage, V_b is the output voltage of the bias voltage supply, and R is the resistance of the InSb detector at the operating temperature. This is a result of changing the resistance of the preamplifier from 100 to 2 M Ω in applying the voltage to the detector. The resistance of the detector is far less than observed in conventional Si and Ge detectors.

The preamplifier output pulses of the InSb detector were observed using a digital storage oscilloscope, and the pulse height spectra were measured using a multichannel analyzer. Most of the measurements were performed without applying any bias voltage in order to avoid the effect of electronic noise. In Fig. 4, typical preamplifier output pulses for some operating temperatures are shown. As seen in Fig. 4(a), all of the contribution to the preamplifier output at 4.2 K was in the form of holes. At higher temperatures, the contributions of both electrons (short time constant) and holes (long time constant) can be seen. We recorded 100 pulses at each of the operating temperatures (except 115 K) and analyzed the contribution of electrons. Examples of measured energy spectra of the alpha particles are shown in Figs. 5(a)–5(e). Measurements were carried out for 5 min at each of the operating temperatures.

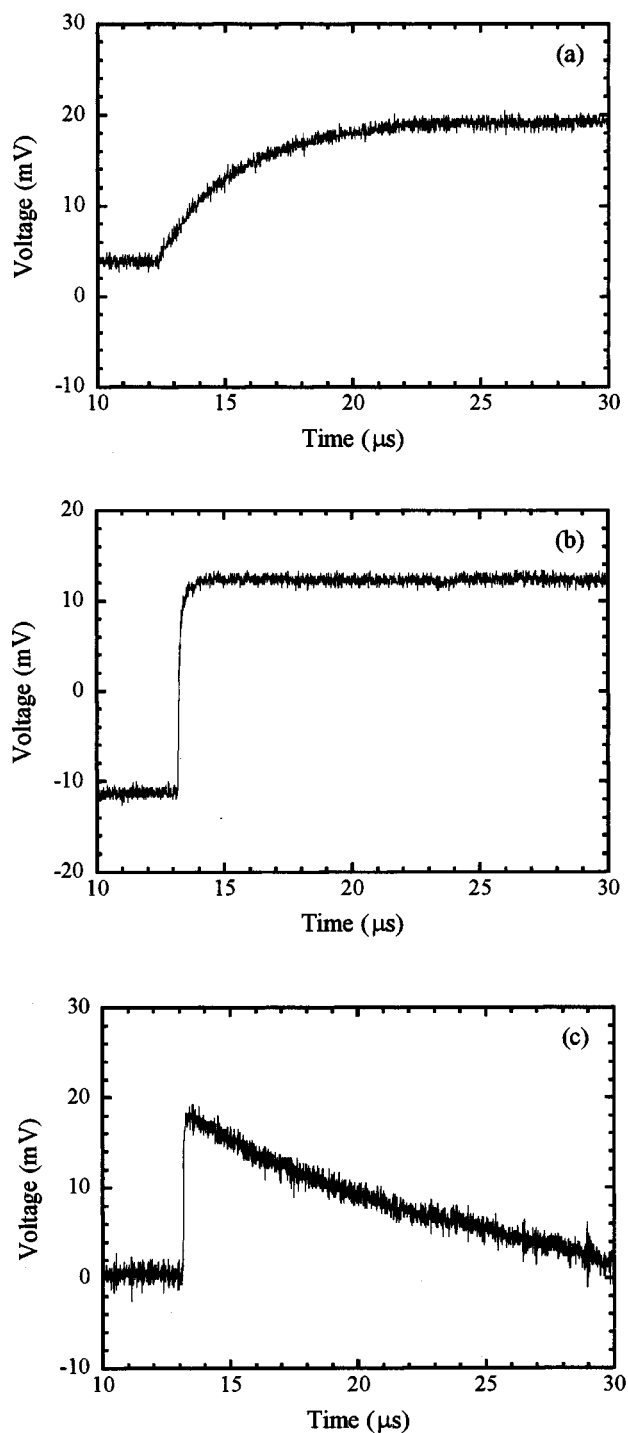


FIG. 4. Preamplifier output pulses at temperatures of (a) 4.2 K, (b) 10 K, and (c) 77 K.

III. DISCUSSION

A. Electric feature of the InSb detector

Comparing with the I - V curves of the previous work (Fig. 2 of Ref. 2), the values of the currents were three orders of magnitude smaller, i.e., the resistances at each operating temperature were 1000 times greater than previously reported. This result does not imply that the pn junction-type detector is superior to the Schottky-type one, but indicates that the fabrication technique is improving. In Fig. 3, a change in resistance of nearly one order of magnitude is

observed between 10 and 15 K. This behavior is very similar to the previous result, although the magnitude of the change is smaller.

B. Output pulses of the preamplifier

As seen in Fig. 4, the output pulses of the preamplifier vary remarkably as the operating temperature changes. In Figs. 4(b) and 4(c), two components are observed in the rising part of the pulses: the fast component is due to electrons, and the slow one is due to holes. We can conclude that all of the voltage was induced by the holes at 4.2 K and mainly as a result of electrons at 77 K.

As will be discussed later, the plasma columns created by the incident alpha particles passed through the depletion layer of the InSb detector. Electrons and holes made a column from the topside of the depletion layer to the bottom-side. The voltage is induced by the movements of electrons/holes to the positive/negative electrodes, respectively. Electrons and holes should contribute one half of the induced voltage, in the case where no capture and trapping of carriers occurs. Contrary to this ideal condition, holes contributed 100% at 4.2 K and electrons had a greater contribution than holes at 77 K and above. This indicates that the electron traps worked at 4.2 K, lost their efficiency at 10 K and above, and that the hole traps were effective at 77 K and above.

For the determination of the kind and energy levels of the carrier traps, deep-level transient spectroscopy is a powerful method. The determination of traps will enable us to find a method of improving InSb substrates.

C. Energy spectra of alpha particles

The energy spectra measured by the pn junction-type InSb detector are different from the ones observed using a Schottky-type InSb detector (Fig. 6 of Ref. 2). In the case of pn junction detectors, an incident charged particle loses some energy before it enters the depletion layer of the detector. Some of the carriers created in the nondepleted region sneak into the depletion layer under the weak electric field, resulting in a complicated energy spectrum. For future x-ray measurements, however, the nondepleted region does not have much of an affect, except attenuating the flux of x rays.

In Fig. 5(a), energy spectra measured with the shaping times of 0.5 and 5 μ s are shown. Due to the long time constant of the pulses of the preamplifier output at 4.2 K, the longer shaping time is effective for charge collection. Comparing the energy spectra of 4.2 K and the ones at higher temperatures, the measured energy of alpha particles is very small at 4.2 K. This is a result of the electrons not contributing at this temperature.

The energy spectra at operating temperatures from 10 to 77 K do not show significant changes. However, events with higher pulse heights dominate at 20 K and the peak at channel number 300 becomes large as the temperature rises, and it disappears at 50 K. At temperatures of 30 K and above, another peak at channel number 180 becomes dominant. This change in peak position corresponds to the contribution of the electrons and holes to the induced voltage, as shown in Fig. 6: from 10 to 40 K, both electrons and holes contribute

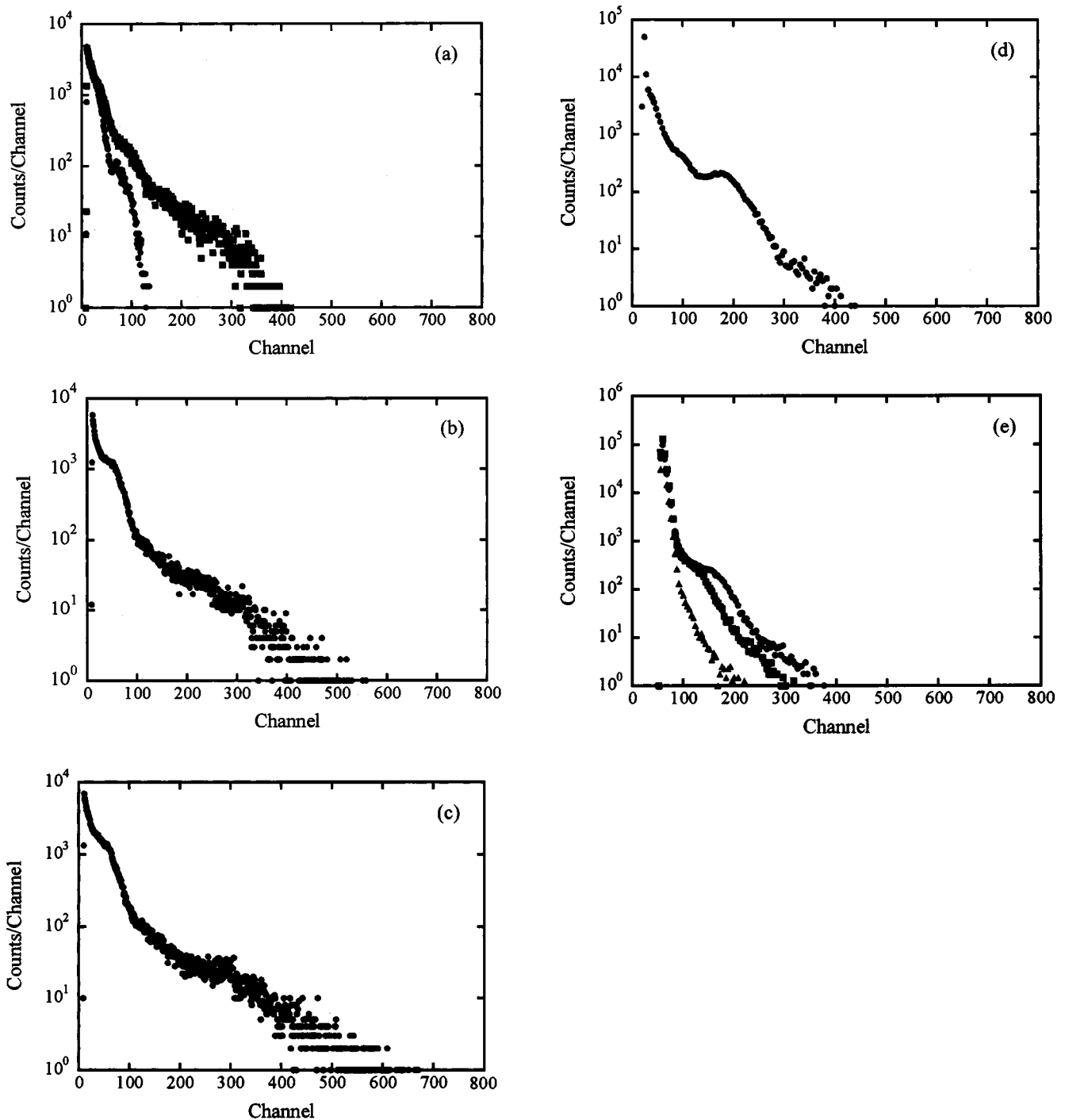


FIG. 5. Energy spectra of ²⁴¹Am alpha particles measured at (a) 4.2 K with shaping times of 0.5 μs (solid circles) and 5 μs (solid squares), (b) 10 K, (c) 20 K, (d) 77 K, (e) 95 K (solid circles), 105 K (solid squares), and 115 K (solid triangles). All measurements were performed without applying a bias voltage. The shaping time for the measurements of (b)–(e) was 0.5 μs.

to the charge collection. However, at temperatures above 50 K, the contribution of holes becomes less. As shown in Fig. 7, noise increases as the temperature rises and the dead-time rate due to thermal noise becomes higher.

At temperatures above 77 K, the pulse heights shift to smaller channel numbers. This phenomenon is explained by the increase in hole density at higher temperatures. As the density of holes increases, the depletion layer thickness *d* becomes thin, as shown by the following equation:

$$d \propto \sqrt{\mu_h \rho V_d} \propto \sqrt{V_d / n_h}, \tag{2}$$

where, μ_h is the mobility of the holes, ρ the resistivity of the InSb substrate, and n_h is the density of the holes.³ A thinner depletion layer results in less energy deposition by alpha particles and makes pulse heights small. This is encouraging in terms of the possibility of operating InSb detectors at temperatures higher than 77 K, making InSb wafers with higher resistivity, i.e., with a lower carrier density.

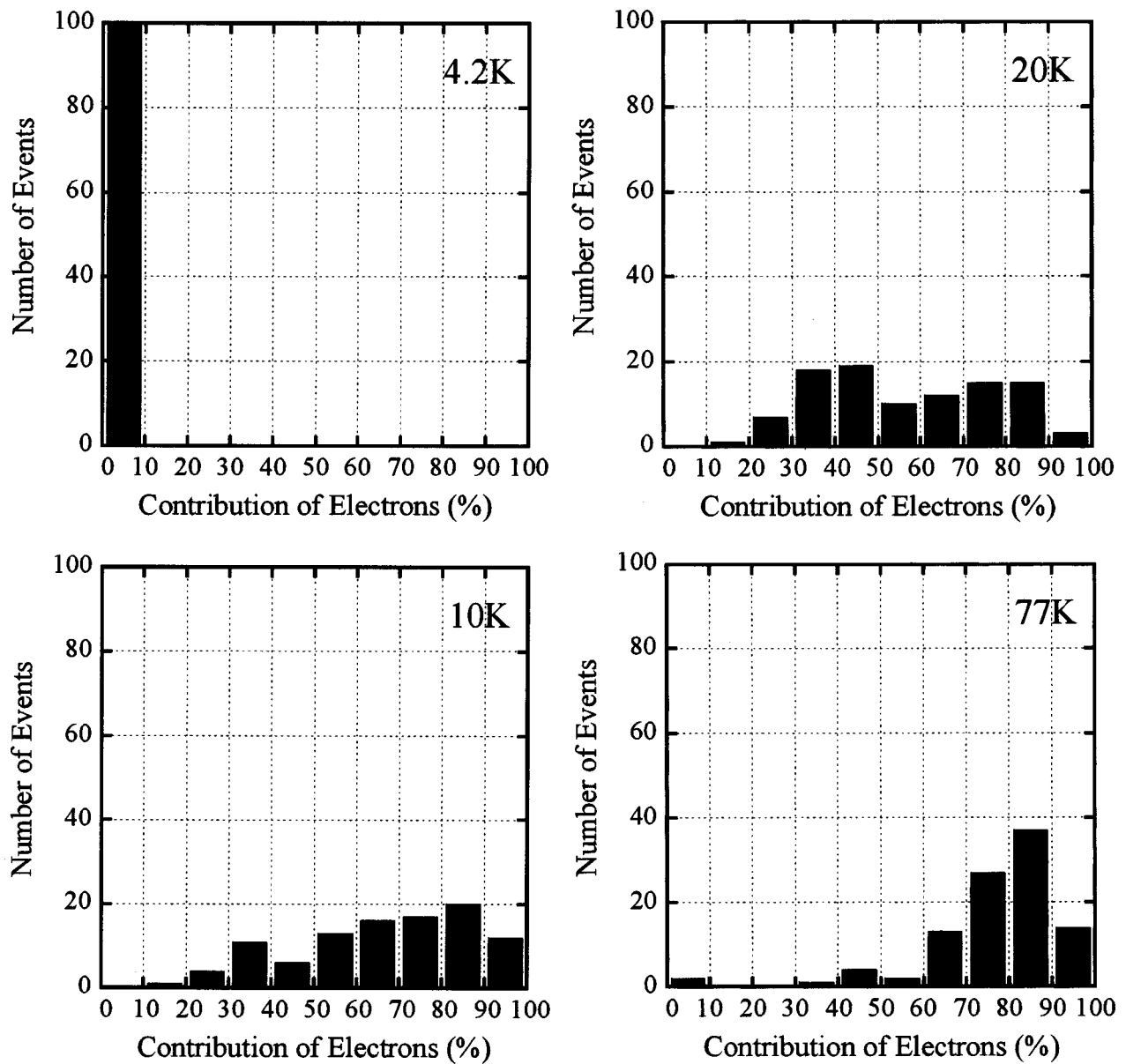


FIG. 6. Examples of the estimated contributions of electrons in the preamplifier output. The operating temperatures are shown in the figures.

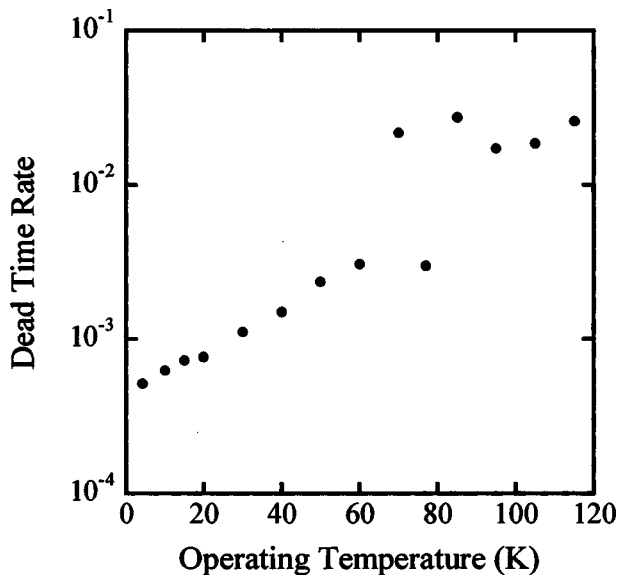


FIG. 7. Dead-time rate as a function of operating temperature.

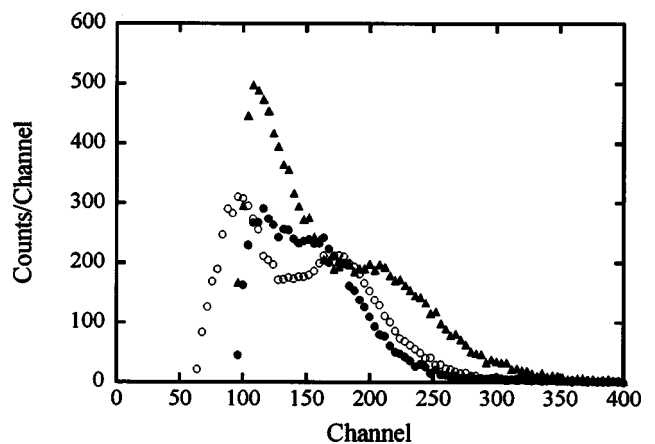


FIG. 8. Examples of the energy spectra of ^{241}Am alpha particles measured at 77 K applying bias voltages of -100 V (solid circles), 0 V (open circles), and $+100$ V (solid triangles), after subtracting noise. The voltage actually added to the InSb detector with the bias voltage is calculated using the second term of Eq. (1), and 0.17 V for the bias voltage of 100 V.

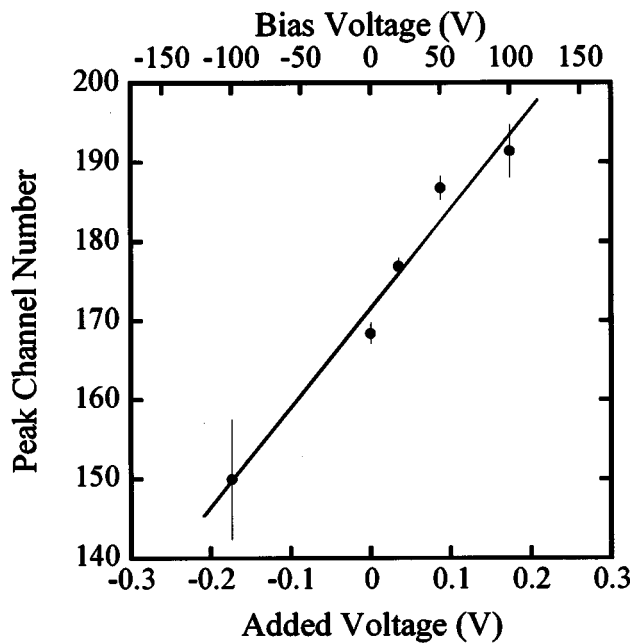


FIG. 9. Peak channel numbers of energy spectra as a function of applied bias voltage. Solid line shows the result of the fitting.

D. Estimation of inherent voltage

Despite the increase in noise, we performed measurements of the energy spectra for bias voltages of -100, 0, 20, 50, and 100 V, at an operating temperature of 77 K. By subtracting noise at the lower channels, we obtained energy spectra with two obvious peaks. Examples of the spectra are shown in Fig. 8. Among these peaks, we employed the peaks with higher channel numbers in each energy spectrum to estimate the effect of applied bias voltage: the peaks at the lower channel numbers may suffer from the influence of the ambiguity in noise subtraction. The obtained peak channel numbers are shown in Fig. 9 as a function of the applied bias voltage. The voltage added to the detector is calculated from the second term of Eq. (1) with a resistance of 20.9 kΩ for the InSb detector at 77 K. The solid line in Fig. 9 is the result of fitting the data.

As described above, the plasma columns created by alpha particles penetrated the depletion layer. A schematic drawing of the depletion layer and the plasma column is shown in Fig. 10. As the voltage added to the detector is

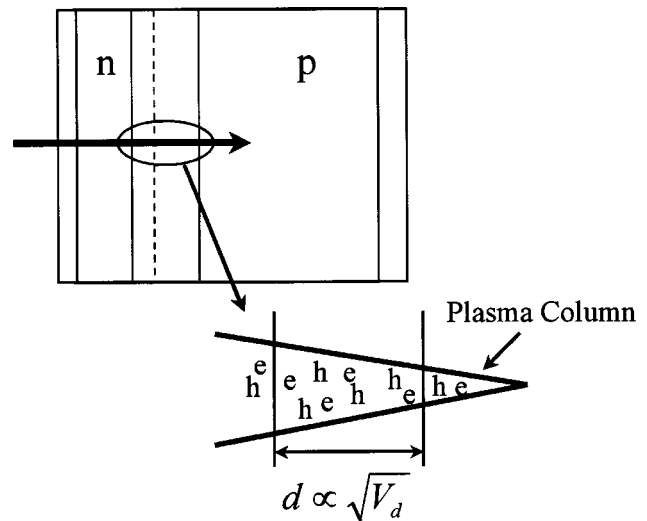


FIG. 10. Schematic drawing of the depletion layer of the InSb detector and the plasma column created by an incident alpha particle. The letters “e” and “h” represent electrons and holes.

small, as calculated by Eq. (1), and the inherent voltage is in the order of 1 V^2 , the change in the depletion layer thickness should be small. We can assume that the peak channel number (measured energy) is proportional to the number of electron-hole pairs created in the depletion layer, i.e., the thickness of the depletion layer. Here, we rewrite Eq. (2) substituting Eq. (1) as

$$d \propto \sqrt{V_d} = \sqrt{V_i} \sqrt{1 + a \frac{V_b}{V_i}} \approx \sqrt{V_i} \left(1 + \frac{a}{2} \frac{V_b}{V_i} \right), \tag{3}$$

where a is the voltage dividing ratio of the second term of Eq. (1). At the point where the fitted line crosses the x axis, the depletion layer thickness is zero. From this we found that the inherent voltage V_i was 0.68 V.

ACKNOWLEDGMENTS

Part of this work was performed with the support of the Venture Business Laboratory Project, Kyoto University.

¹W. C. McHarris, Nucl. Instrum. Methods Phys. Res. A **242**, 373 (1986).
²I. Kanno, F. Yoshihara, R. Nouchi, O. Sugiura, T. Nakamura, and M. Katagiri, Rev. Sci. Instrum. **73**, 2533 (2002).
³G. F. Knoll, *Radiation Detection and Measurements* (Wiley, New York, 2000).